Journal of Marine Systems 245 (2024) 103990

Contents lists available at ScienceDirect

Journal of Marine Systems

journal homepage: www.elsevier.com/locate/jmarsys

The Fujiwhara effect on ocean biophysical variables in the southeastern tropical Indian Ocean region

Riza Yuliratno Setiawan [a,*], R. Dwi Susanto [b,c], Takanori Horii [d], Inovasita Alifdini [e], Eko Siswanto [d], Qurnia Wulan Sari [f], Anindya Wirasatriya [g], Candra Aryudiawan [a]

[a] Department of Fisheries, Faculty of Agriculture, Universitas Gadjah Mada, Yogyakarta, Indonesia
[b] Department of Atmospheric and Oceanic Science, University of Maryland, College Park, MD 20742, USA
[c] Marine Estuarine and Environmental Sciences, University of Maryland, College Park, MD 20742, USA
[d] Japan Agency for Marine-Earth Science and Technology (JAMSTEC), Japan
[e] Institute of Meteorology and Climate Research, Karlsruhe Institute of Technology, Karlsruhe, Germany
[f] Department of Marine Science, Faculty of Fisheries and Marine Science, Padjadjaran University, Bandung, Indonesia
[g] Department of Oceanography, Faculty of Fisheries and Marine Science, Diponegoro University, Semarang, Indonesia

ARTICLE INFO

Keywords:
Tropical cyclone
Fujiwhara effect
Remote sensing
Phytoplankton
Upwelling
Chlorophyll-a
Southeastern tropical Indian Ocean (SETIO)
Indonesian throughflow

ABSTRACT

A rare event known as Fujiwhara effect occurred in the southeastern tropical Indian Ocean when tropical cyclones (TCs) Seroja and Odette were co-existed, interacted each other, and merged into one TC in April 2021. Here, remotely sensed data (surface winds, sea surface temperature, chlorophyll-a concentration, and surface currents) were analyzed to determine the impact of Fujiwhara effect on the ocean biophysical variables in the region. Ekman pumping velocity were computed to determine the upwelling/downwelling process. During the entire development of the TCs to the merging, the TCs induced sea surface temperature (SST) cooling and raising sea surface chlorophyll-a. Ekman pumping and inertial pumping may serve as the primary driving force for the observed negative SST anomaly and positive anomaly in chl-a concentration associated with TCs. This rare event adds the complexity of ocean and climate dynamics of the region as an exit gate of the Indonesian throughflow to the Indian Ocean and may have implications to circulation and climate in the Indian Ocean and beyond. The present research likely represents the first scientific documentation of oceanic responses to a Fujiwhara effect in the region.

1. Introduction

Tropical cyclones (TCs) are recognized by several terms in distinct regions of the world, such as cyclones, hurricanes, and typhoons. Depending on where they occur, cyclones (South Pacific and Indian Ocean) are also referred to as hurricanes (Atlantic and the Northeast Pacific region) or typhoons (Northwest Pacific). Tropical cyclones (TCs) are strong rotating vortices of air at synoptic region scale that has been approved as the indication for the impact of climate change, increasing of surface ecological, and environmental damage (Busireddy et al., 2019; Hung and Gong, 2011; Knutson et al., 2020; L. Liu, 2013; Siswanto et al., 2008; Wang, 2020; Wu et al., 2019; Zhang et al., 2020, 2021).

Our observation area covers the southeastern tropical Indian Ocean (SETIO) region extending from the western Sumatra Island to the Lesser Sunda Island (Fig. 1) with latitudinal position from 0° to 20°S and longitudinal location from 80°E to 130°E. There have been some TCs occurred in this region, for examples TC Bakung (2014) near south Sumatra water, TC Cempaka (2017) near East Java, TC Dahlia (2017) southwest Java waters and TC Seroja (2021) near Savu Sea (Paterson, 2012; Yang et al., 2020; Samodra et al., 2020; Aditya et al., 2021; Setiawan et al., 2021). In April 2021, for the first time in the SETIO region, two TCs (TC Seroja and TC Odette) occurred at the same time, close and interact each other, and eventually merged together which known as Fujiwhara effect (Fujiwhara, 1921, 1922, 1923, 1931). The uncommon phenomenon (Fujiwhara effect) occurs when two TCs move towards each other and when the distance is <900 km, the two TCs will begin to circulate around each other and eventually merge. The two TCs will be eventually merged with stronger TC absorbs the weaker TC. If the two TCs have equal strength, they may merge into a common center or moving off into separate paths (Fujiwhara, 1921, 1923).

* Corresponding author.
E-mail address: riza.y.setiawan@ugm.ac.id (R.Y. Setiawan).

https://doi.org/10.1016/j.jmarsys.2024.103990
Received 22 October 2023; Received in revised form 25 May 2024; Accepted 27 May 2024
Available online 28 May 2024

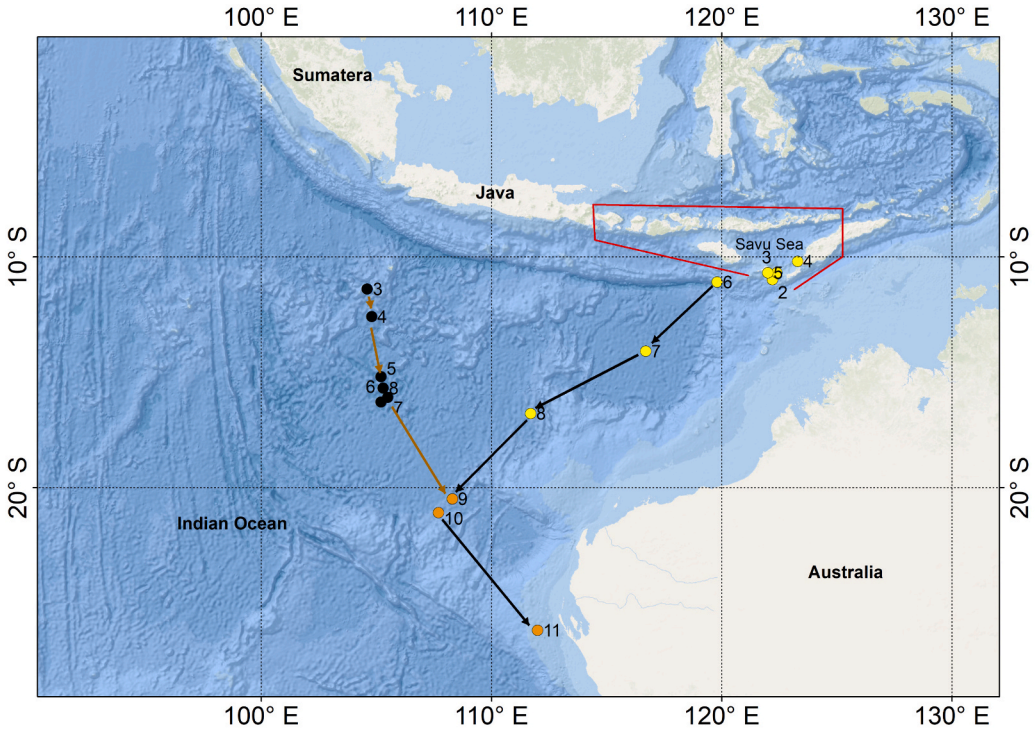

Fig. 1. Map of area of interest. Black and yellow dots demonstrate the tracks of TCs Odette dan Seroja. Brown dots indicate the track of Fujiwhara effect. Magenta line denotes the Lesser Sunda Island. Numbers indicate the date of April 2021. (For interpretation of the references to colour in this figure legend, the reader is referred to the web version of this article.)

Several previous studies addressed the dynamics of the interaction between two cyclones/Fujiwhara effect (i.e., DeMaria and Schubert, 1984; Demaria and Chan, 1984; Liou et al., 2019; Liou and Pandey, 2020; Fu et al., 2018; Dong and Neumann, 1983; Lee et al., 2023; Ito et al., 2023). However, research on the effects of the Fujiwhara effect on ocean biophysical variables has not been explored. TC passing over the oceans is expected to cause subsurface colder water and marine phytoplankton lift to the surface, as a result cooling the sea surface temperature (SST) and raising the sea surface chlorophyll-a (chl-a) concentration. Since global warming may increase the intensity and frequency of TCs (Pandey et al., 2021; Zhao et al., 2015), further understanding their impacts on ocean biophysical variables is needed. Given the significant and ongoing Indian Ocean warming (Sharma et al., 2023), it is also important to show how the ocean responds to recent extreme TCs. The ocean biophysical variable of chl-a concentration is a crucial marine index and productivity. It plays an important role in the process of material cycle and energy conversion in the marine ecological system, of relevance to marine atmospheric carbon cycle in the system, environment monitoring, ocean dynamics (upwelling and coastal current), and fishery management (Behrenfeld and Falkowski, 1997; Hout et al., 2007; Roxy et al., 2016). Thus, many researchers who focus on the ocean, atmosphere, and the environment believe that chl-a concentration is an important parameter in the study of ocean colour and marine ecological environment. In recent years, researchers studied influences of TCs on the ocean biophysical parameters and roles of TCs' translation speed and forcing time in phytoplankton blooms (e.g., Lin et al., 2003; Setiawan et al., 2021). By using ocean colour remote sensing data, many studies showed that the cause of blooms in the offshore area is a series of physical processes, like upwelling, strengthened mixing and entrainment, which all increase sea surface nutrients during the TCs (Chen and Tang, 2012; Lee et al., 2020; F. Liu and Tang, 2018; Zhao et al., 2008, 2013).

The physical mechanism for the increase in chl-a concentration is that TC winds induce mixing and upwelling, which bring subsurface nutrient into the euphotic zone. In addition, TCs-induced increase in chl-a concentration depends on the amount of subsurface nutrients brought to the surface by upwelling (Busireddy et al., 2019; Islamiyah et al., 2023; Lin et al., 2003; Setiawan et al., 2021; Windupranata et al., 2019; Zhang et al., 2020). The effect of TC Seroja on ocean biophysical variables has been reported previously by Setiawan et al. (2021), however the Fujiwhara effect of two TCs Seroja and Odette that merged into stronger TC and its impacts on the ocean biophysical parameters have not been studied before. In the case where two typhoons locate close to each other, it is expected that there are two peaks of negative wind stress curl that produce strong Ekman upwelling, and an opposite peak of Ekman downwelling between them. Hence, motivated by previous investigators cited above, our primary goal is to evaluate the response of ocean biophysical variables during the interactions between TCs Seroja and Odette and subsequent merged into a single stronger TC using remote sensing data.

2. Data and methods

2.1. Study area

The study area is the southeastern of the Indian Ocean (SETIO) region from 0° to 30°S and from 80°E to 130°E, located between Indonesia and Australia (Fig. 1). The SETIO region is dynamically complex due to several oceanic-atmospheric processes occurred in the region such as the Indonesian throughflow (ITF), oceanic Kelvin and Rossby waves, oceanic eddies, Madden Julian Oscillation (MJO), monsoon induced upwelling, Indian Ocean Dipole (IOD), and El Niño-Southern Oscillations (ENSO). The SETIO region is a junction of Kelvin waves originated from the equatorial Indian Ocean that propagate along the southern coasts of the Lesser Sunda Island Chains from Sumatra to Timor, Rossby waves from the Pacific Ocean that propagate along the western coast of Papua, and the ITF. In addition, thermocline eddies are known to develop in this region to add to the complexity of ocean dynamics of the

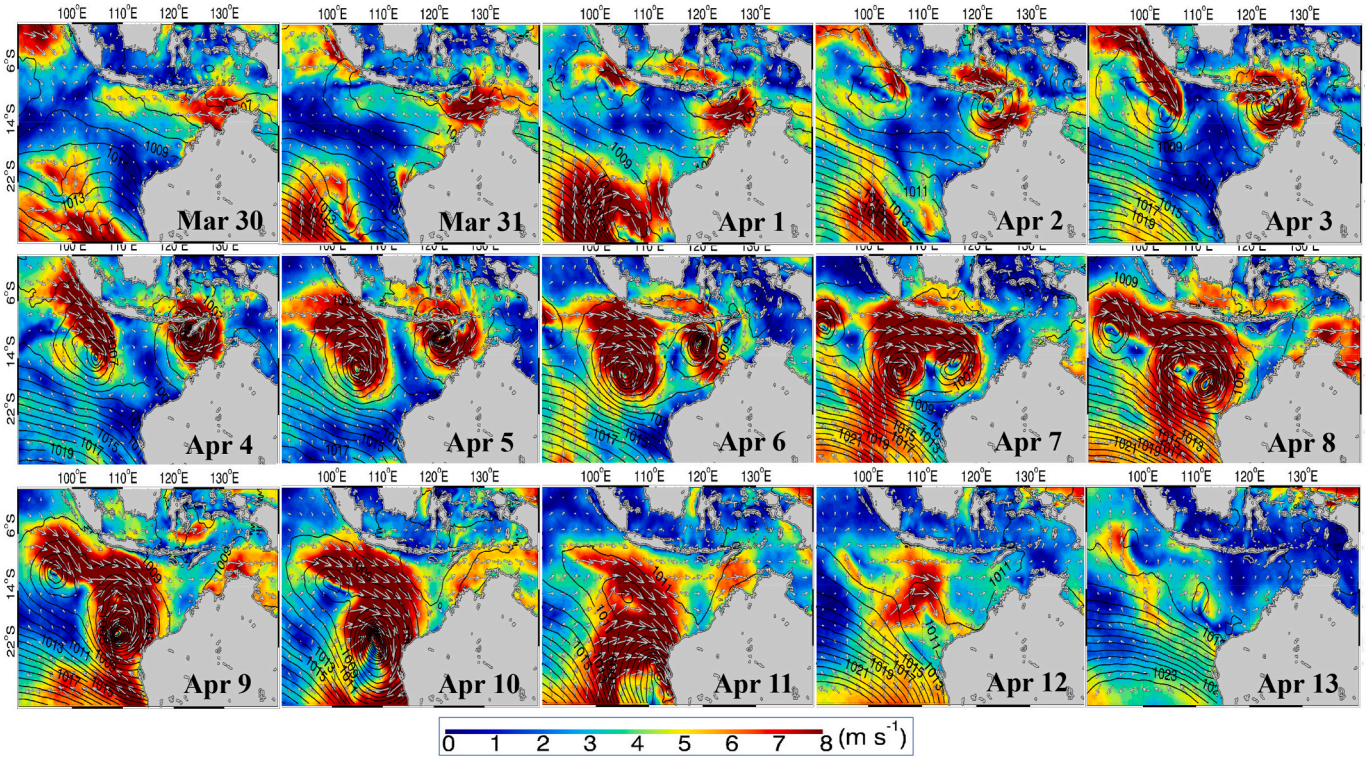

Fig. 2. Map of daily wind speed anomaly relative to the 2015–2021 mean (colour) overlaid with wind direction (arrow) from March 30 to April 13, 2021, in the SETIO region. Black contour lines depict sea level pressure (SLP).

SETIO region.

The region is strongly influenced by the Australia-Indonesia monsoon system and modulated by IOD and ENSO. In term of the chl-a concentrations, the monsoonal winds-induced upwelling occurs along the southern coasts of the Lesser Sunda Island chain, and mostly concentrate in the south Java-Sumatra during the Austral winter and modulated by IOD and ENSO (i.e., Susanto et al., 2001; Iskandar et al., 2022; Mandal et al., 2022). In contrast, the chl-a concentrations in the deep-sea/open sea region are relatively low. The region is also known as the center for Indian Ocean tuna hatching (e.g., Nugroho et al., 2023).

2.2. Data

This study used satellite remote sensing data to analyze the changes in SST, wind speed, and surface chl-a concentration during the interaction of TCs Seroja and Odette through the Fujiwhara effect. The wind stress (τ) on the ocean surface and the Ekman Mass Transport (EMT) were calculated by employing the equation of Hsieh and Boer (1992). To understand the physical forcing of both TCs, the surface wind data obtained from the Cross-Calibrated Multi-Platform (CCMP) gridded surface vector winds version 2.0 for the period of 30 March-15 April 2021 were analyzed. The CCMP used is a level-3 ocean wind vector products generated from various satellites, moored buoy, and model wind data. The dataset can be downloaded from https://www.remss.com/measurements/ccmp/ (accessed on September 9, 2021). The surface wind spatial and temporal resolutions are $0.25^{o} \times 0.25^{o}$ and every six hour, respectively. The accuracy of the CCMP is higher than the other wind reanalysis data (Atlas et al., 2011).

To observe the ocean response to TCs, we used the Ocean Surface Current Analysis-Real Time (OSCAR) data (Bonjean and Lagerloef, 2002). The daily dataset on 1/4° × 1/4° grid were downloaded from Physical Oceanography Distributed Active Archive Center at the Jet Propulsion Laboratory of NASA (https://podaac.jpl.nasa.gov/dataset/OSCAR_L4_OC_third-deg). We also used in situ vertical profiles of temperature and salinity measured by an Argo float to investigate changes in the ocean vertical structure associated with the passage of the TCs. The Argo data were obtained from the advanced automatic quality control Argo Data prepared by the Japan Agency for Marine-Earth Science and Technology (http://www.jamstec.go.jp/ARGO/argo_web/argo/?page_id=100&lang=en). After checking the quality-control flag of each profile, we used the data for 0–300 m. We interpolated the profiles vertically to every 1 m using the Akima spline method (Akima, 1970). Because a lot of data above 5 m were missing values, we used the values at 6 m as the top layer.

2.3. Method

To obtained better indication of the upwelling strength, we also calculated the Ekman Pumping Velocity (EPV) by using the following formula (Wang and Tang, 2014; Wirasatriya et al., 2020):

$$\boldsymbol{EPV} = -curl_z\left(\frac{\boldsymbol{\tau}}{\boldsymbol{\rho_w f}}\right) \quad (1)$$

where

$$curl_z(\tau) = \frac{\partial \tau_y}{\partial x} - \frac{\partial \tau_x}{\partial y} \text{and } \tau = \rho_a C_d U_{10}^2 \quad (2)$$

where τ is wind stress, $\boldsymbol{\rho_a}$ is the density of air (1.25 kg m^{-3}), ρ_w is the density of seawater (1025 kg m^{-3}), $\boldsymbol{C_d}$ is the drag coefficient, $\boldsymbol{U_{10}}$ is the wind speed 10 m above sea level, and f is the Coriolis parameter (Stewart, 2008). To determine the drag coefficient, we used the following equations (The, 1988):

$$1000C_d = 1.29 \text{ for } 0 < U_{10} < 7.5\ m\ s^{-1} \quad (3a)$$

$$1000C_d = 0.8 + 0.0065\ U_{10} \text{ for } 7.5 < U_{10} < 50\ m\ s^{-1} \quad (3b)$$

Moreover, the hourly sea level pressure (SLP) data was obtained from the European *Re*-analysis (ERA-5) produced by the European Centre for Medium-Range Weather Forecasts (ECMWF) with a grid

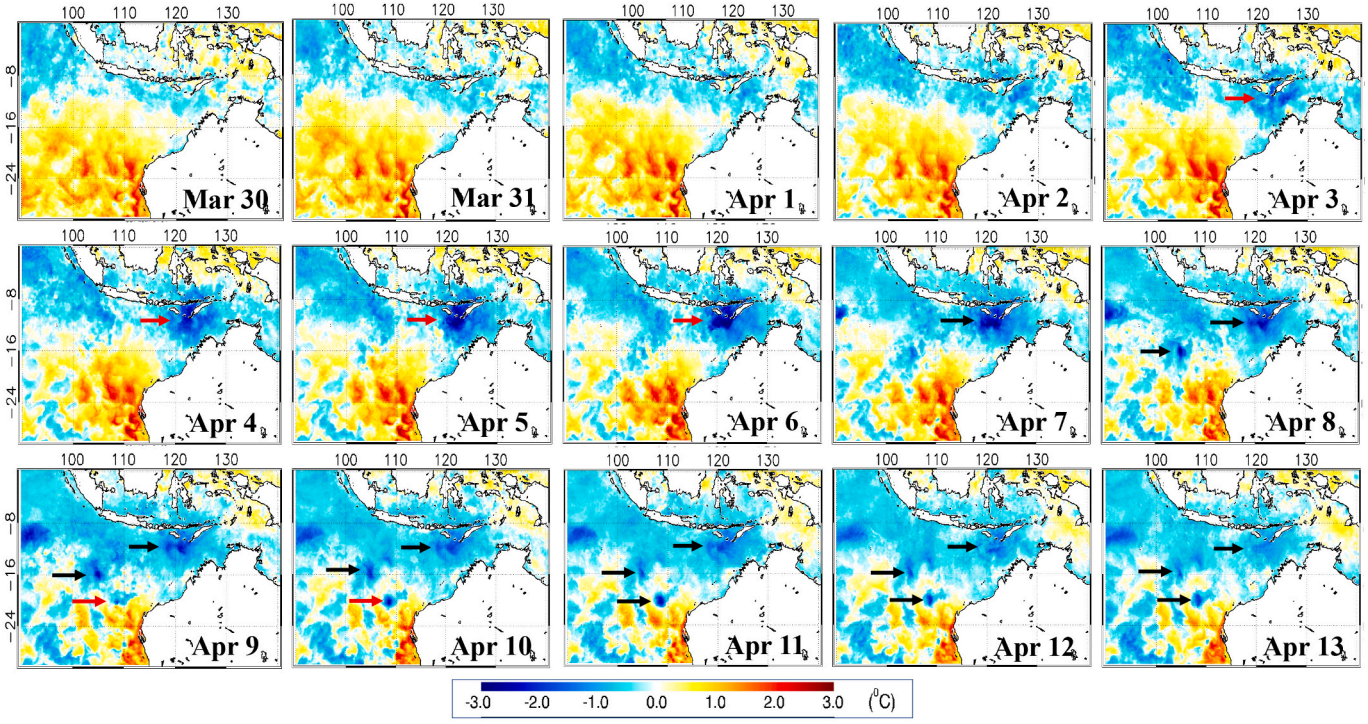

Fig. 3. Map of daily sea surface temperature (SST) anomaly (relative to the 2015–2021 mean) from March 30 to April 13, 2021, in the SETIO region. Red (black) arrows denote the dominant forcing, which is Ekman pumping (inertial pumping). (For interpretation of the references to colour in this figure legend, the reader is referred to the web version of this article.)

interval of 0.25° (Hersbach et al., 2020). The data are available at https://cds.climate.copernicus.eu/cdsapp#!/dataset/reanalysis-era5-single-levels?tab=overview (accessed on June 3, 2021). The hourly data were averaged into daily data.

In order to determine the presence and intensity of upwelling, the Optimally Interpolated (OI) SST Remote Sensing System data were analyzed (http://www.remss.com/measurements/sea-surface-temperature/) (accessed on September 9, 2021). Specifically, the 9 km

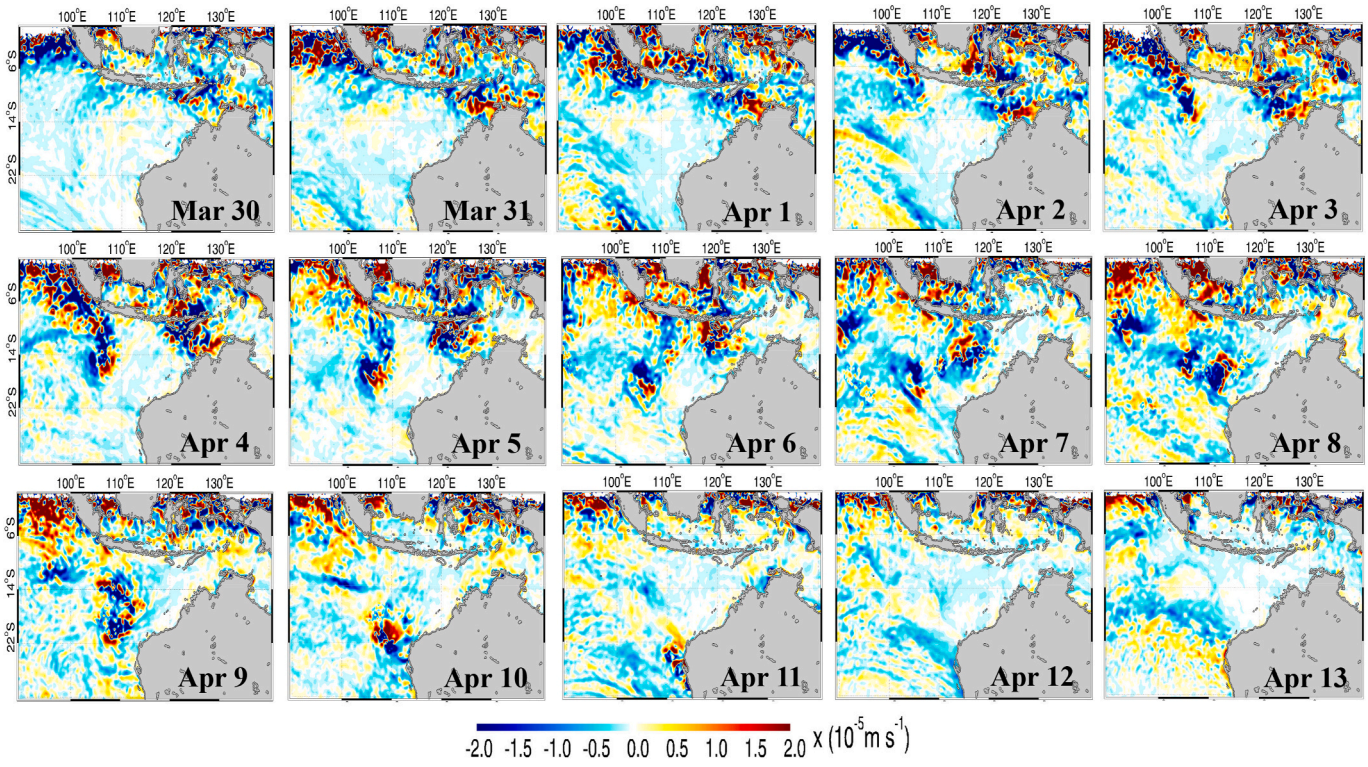

Fig. 4. Map of the daily Ekman Pumping Velocity (EPV) anomaly (relative to the 2015–2021 mean) from March 30 to April 13, 2021, in the SETIO region. A negative (positive) EPV anomaly indicates upwelling (downwelling).

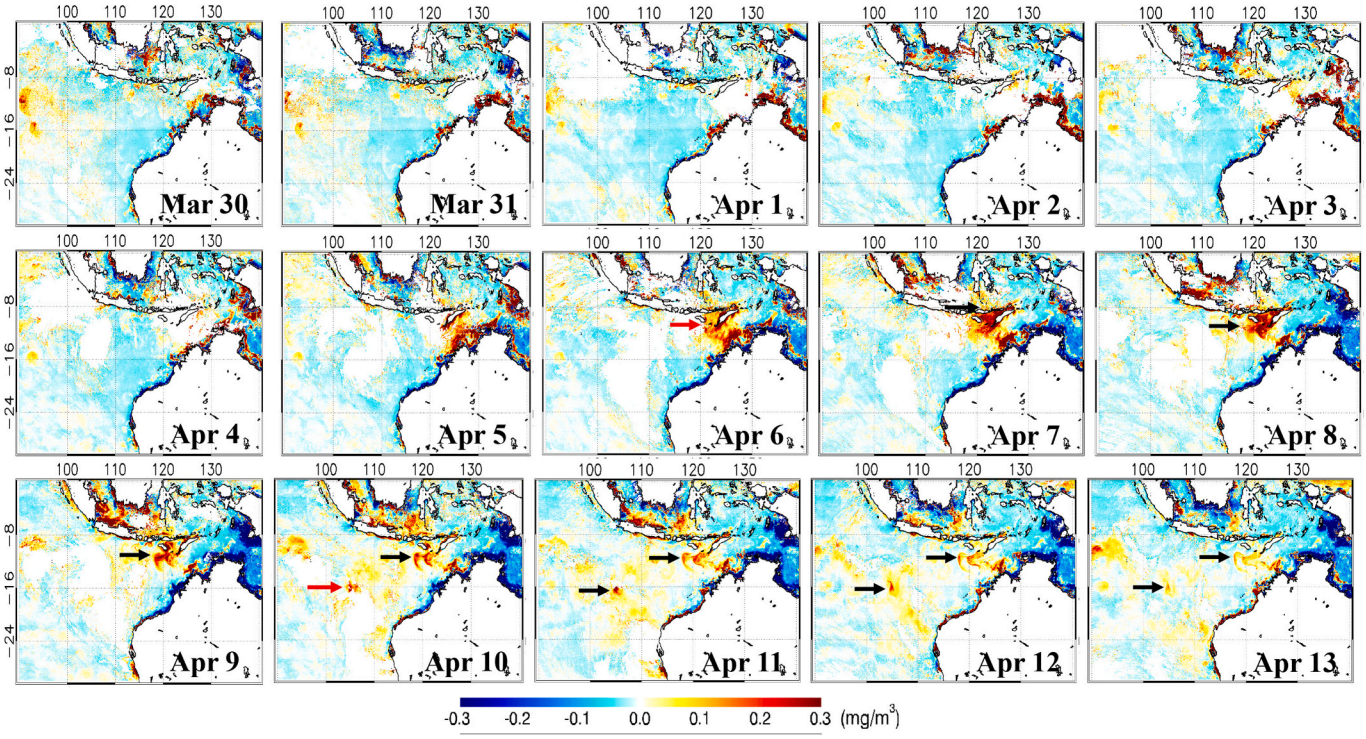

Fig. 5. Map of daily surface chlorophyll-a anomaly (relative to the 2015–2021 mean) from March 30 to April 13, 2021, in the SETIO region. Red (black) arrows denote the dominant forcing, which is Ekman pumping (inertial pumping). (For interpretation of the references to colour in this figure legend, the reader is referred to the web version of this article.)

microwave-infrared OI SST product was utilized to distinguish the SST responses during the TCs Seroja and Odette events.

The surface chl-a data employed to evaluate the response of the biomarine indicator in this research is a daily satellite image of the Himawari-8 Level 3 (https://www.eorc.jaxa.jp/ptree/) (accessed on June 3, 2021). The image has a spatial resolution of 5 × 5 km and a daily temporal resolution (Murakami, 2016). The daily surface chl-a data from 30 March to 13 April 2021 were analyzed to examine the impact of TCs Seroja and Odette on phytoplankton chl-a concentrations.

To better evaluate the Fujiwhara effect from TCs Seroja and Odette on the ocean biophysical parameters, the daily anomaly of surface wind speed, chl-a concentration, SST, and EPV from 30 March to 13 April 2021 were evaluated to represent prior, during, and after the passages of TCs Seroja and Odette. As a baseline, climatological calculations from 2015 to 2021 were performed. Meanwhile, the daily temperature anomaly of the ARGO float was defined as the temperature difference from the mean temperature averaged for 14 March-23 April 2021.

3. Results and discussion

A robust effect of TC Seroja on ocean biophysical variables has been reported by Setiawan et al. (2021), meanwhile the effect of combination of the TCs Seroja and Odette on those parameters is examined in this paper. Fig. 2 reveals the surface wind magnitude superimposed with the SLP. The low SLP system accompanied the high vortex of surface wind. The evolution of dual vortex intensified from 30 March 2021 near western Sumatra and the Savu Sea. On 3 April 2021, TC Odette and TC Seroja formed over the SETIO region and Savu Sea. The low SLP in the Savu Sea exhibited an initial westward movement, followed by a rapid change in direction towards the southwest on the 6th and 7th of April. During 8–9 April, the low SLP in the Savu Sea began to interact with another tropical low SLP from western Sumatra. These two TCs interacted through the Fujiwara effect from 7 to 11 April 2021. TC combination of vortex took a sharp turn towards the southeast and began to accelerate towards the western Australian coast on 9 April. The system further intensified into a severe TC. It weakened on 12 April as it moved further inland and disappeared on 13 April.

Figure 2 illustrates a notable wind anomaly (> 8 m s^{-1}) observed in the SETIO region. Under normal condition, the transitional phase of the Australia-Indonesia monsoon (March–April) in the SETIO region does not support the occurrence of strong wind, SST depression, and phytoplankton bloom. Nevertheless, it is evident that there is a significant SST anomaly observed in the Savu Sea. This anomaly is characterized by a notable decrease in SST, reaching up to 3 °C, which commenced on 3 April, coinciding with the occurrence of intense vortex surface winds and low SLP (Fig. 3). Ocean surface of the Savu Sea experienced this situation until 5 April. The vortex surface winds and low SLP moved southwestward towards the Indian Ocean on 6 April.

The position of TC Seroja center (Fig. 2) and cold SST center (Fig. 3) was similar during TC development, i.e. from 3 to 5 April 2021. Because of the proximity of the TC center to the oceanic response, this suggests that the dominant forcing for the SST depression and perhaps the chl-a maxima (no chl-a data due to cloud cover) in the Savu Sea during the period was Ekman pumping (Suzuki et al., 2011). Positive and negative EPVs indicate a strong downwelling and upwelling process, respectively (Fig. 4). Significant upwelling processes were identified during 2–4 April 2021 in the western Sumatra waters and the Savu Sea. The influence of EPV on the Savu Sea vanished from 7 April, but SST depression still appeared in the sea until 12 April (as denoted by red arrows in Fig. 3). Significant chl-a anomalies (> 0.1 mg m^{-3}) persisted in the Savu Sea from 7 April to 13 April 2021 (denoted by black arrows in Fig. 5). This may simply because the ocean response was delayed by several days. The chl-a anomalies would partly be explained by the effect of oceanic inertial pumping. As shown in Suzuki et al. (2011), the inertial pumping becomes dominant in the case of a fast-moving TC and in such case upwelling maximum appears behind the TC center.

TC Odette and TC Seroja interacted and then merged during 7–9 April 2021, forming the Fujiwhara effect (Fig. 2). There were two

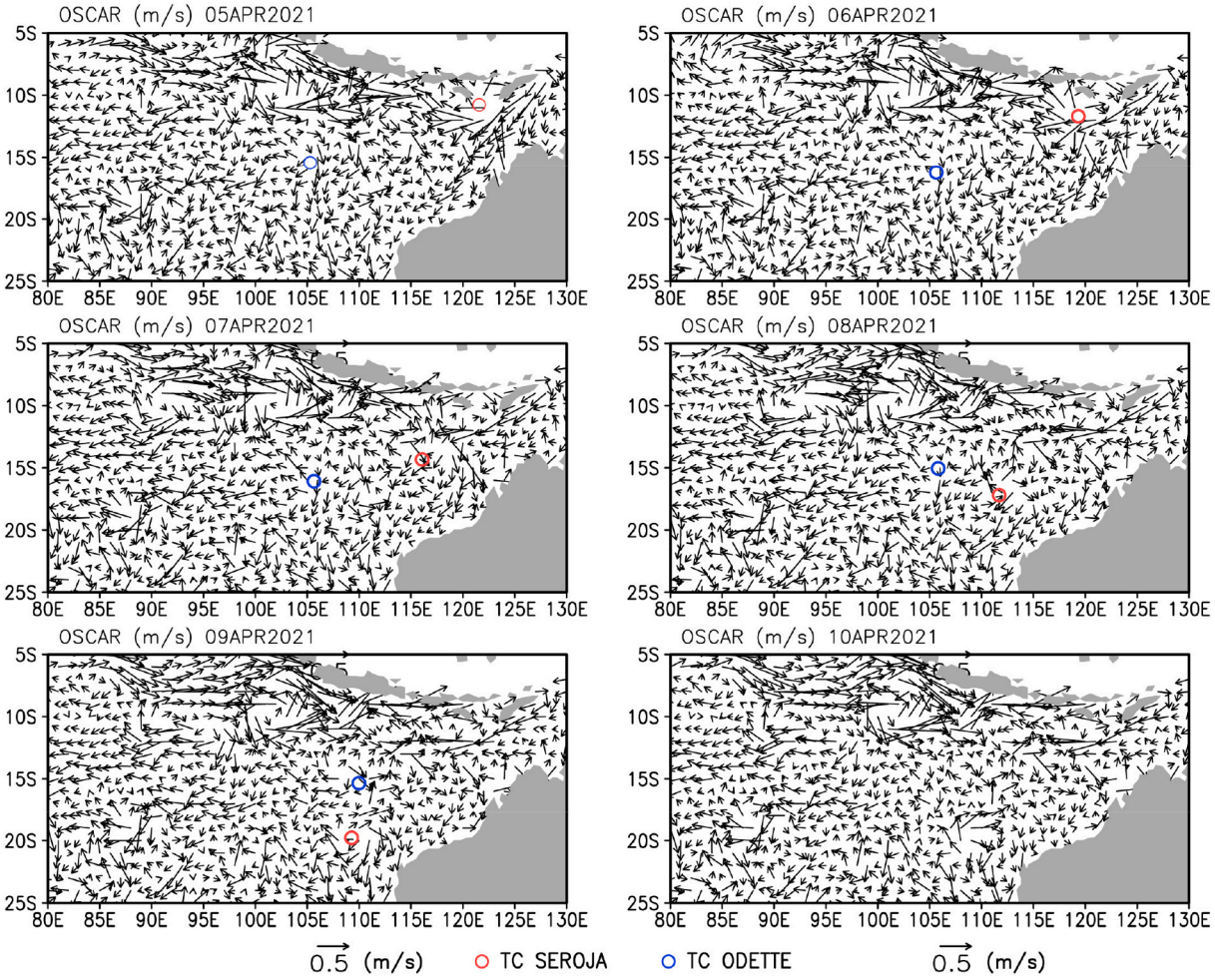

Fig. 6. Snapshots of the estimated ocean surface current (10 m depth) of OSCAR data for 5–10 April 2021. Red and blue circles depict the centres of TC Seroja and TC Odette. (For interpretation of the references to colour in this figure legend, the reader is referred to the web version of this article.)

prominent cold SST cores that occurred during 9–13 April resulting from the two TCs, as shown by black and red arrows in Fig. 3. It is likely that the responsible forcing for these cold SST cores was distinct, i.e. the inertial pumping (Ekman pumping) may have played a major role in the black (red) arrow cold SST core during 9–10 April. Meanwhile, the inertial pumping probably was the dominant forcing for the cores of cold SST and of chl-a maxima (Fig. 5) from 11 to 13 April 2021 (denoted by black arrows) due to the position of the cores behind the TC centers.

A critical feature in understanding ocean primary productivity is surface chl-a variability. The lack of chl-a data in the site was primarily attributed to the presence of cloud cover over the area. We hypothesized that the observed increase in chl-a concentration was caused by pronounced Ekman pumping and inertial pumping, which significantly elevated the nutricline and thermocline in the open ocean. Although the missing data hinder the chl-a variations during the two passages of the TCs (Fig. 5), the persistent two peaks of cold SST and the positive chl-a anomalies are consistent with that the Ekman pumping and the inertial pumping served as the primary driving force for the observed ocean responses.

Ocean response to the two TCs under the Fujiwhara effect would show a complex pattern due to different processes of Ekman pumping and inertial pumping. In case two TCs move clockwise around an area, two Ekman upwelling and a downwelling between them is expected, as a response to wind stress curl between the two TCS. On April 6, patches of positive EPV anomalies (downwelling) around 14°S, 111°E were formed between the two TCs (Fig. 4). From 7 to 9 April, the two TCs interacted and merged with each other moving clockwise around the region (15°-16°S, 108°-111°E) as an indication of the typical Fujiwhara effect (Figs. 1 and 6). For the three days, Positive EPV anomalies between the two TCs were not significant. Rather, positive EPV anomalies were noticeable behind the moving TC Seroja. Ocean surface currents during the period when the TCs were under the Fujiwhara effect (7–9 April) were characterized by two clockwise circulations, or cyclonic eddies, around the center of the TCs (Fig. 6). The circulations were well observed just prior to the TCs's merge on 9 April as the west of the TC Odette center around 15°S, 109°E and around the TC Seroja center. The region between the two TCs was almost stationary (around 15°-16°S, 109°-111°E) over the three days. The region is expected to be a deepening of the thermocline due to Ekman downwelling and convergence of surface currents. In the region, weak positive SST anomalies persisted before the approach and after the passage of the TCs from April 6 to 13 (Fig. 3). The chl-a response is less significant than the SST, but at least no positive chl-a peak occurred, and weak but negative chl-a anomalies were observed on 11 April (Fig. 5). These complex patterns of SST and chl-a anomalies are likely the indication of the ocean response to two TCs under Fujiwhara effect.

Finally, we examined the ocean vertical structure before and after the passage of the TCs by an Argo float (No. 2902789) that nearly stayed around the two TCs. The Argo floats provided profiles about every 10 days during the March–April 2019, enabled us to observe ocean conditions before, during, and after the TC passages (Fig. 7). Here, temperature anomalies were defined as the temperature difference from the mean temperature averaged over the period shown in the Fig. 7. The temperature profiles from the Argo float demonstrate significant rise

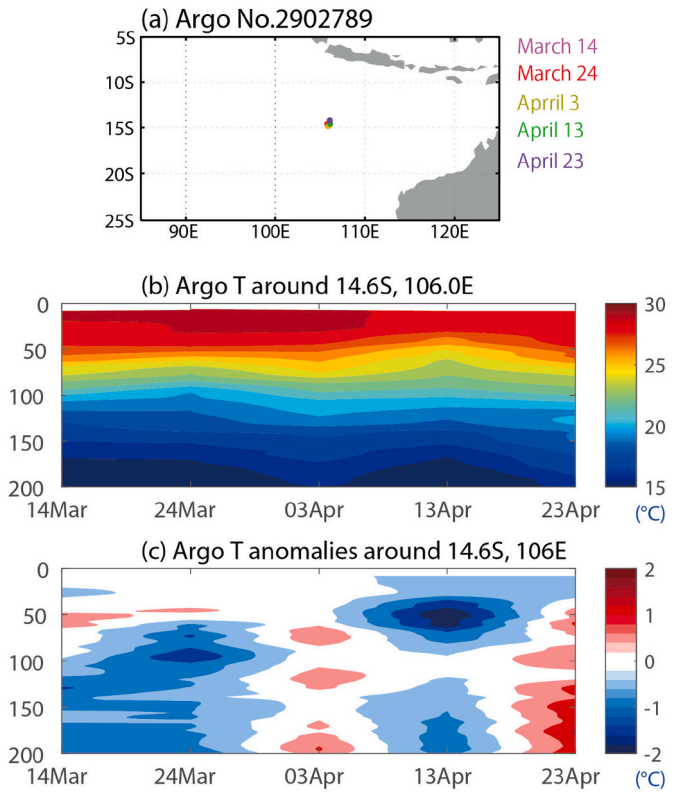

Fig. 7. (a) Observation points of an Argo float (No. 2902789) during 14 March-23 April 2021. (b) Temperature profiles observed by the Argo float. (c) As in Fig. 7b, but for the temperature anomalies. The anomalies were defined as the temperature difference from the mean temperature averaged for 14 March-23 April 2021.

(>20 m) of the top thermocline from April 3 to 13 (Fig. 7b). This would be an upwelling consistent with the basic ocean response under a TC passage. The Argo float probably missed the subsurface downwelling expected from the Fujiwhara effect because the location (around 14.6°S, 106°E) is west of the region that is the center of the Fujiwhara effect and probably observed primarily Ekman pumping.

Present report is probably the first example showing ocean responses to two TCs under the Fujiwhara effect in the Indian Ocean. Although we were unable to show the ocean structure beneath the positive SST and weak chl-a anomalies between the two TCs, we believe that these observational data in the surface and sub-surface ocean presented here will provide useful information for future numerical modeling studies.

4. Conclusions

The present work revealed that the Ekman pumping and inertial pumping may have played a dominant role for the ocean biophysical variables in response to the interaction between dual TC Seroja and TC Odette that merged into a single stronger TC, which is known as the Fujiwhara effect. When the core positions of TC and of cold SST and chl-a maxima are distinct, the dominant process for the cooling and the bloom is likely the inertial pumping. In contrast, our results suggest that when the TC core, cold SST, and chl-a maxima are close to each other the dominant process is Ekman pumping. Further research is needed to determine how ocean vertical structure develops between the TCs and their two upwelling peaks under the Fujiwhara effect. Understanding the dominant mechanism induced by this rare event in this area is essential for improving the knowledge of ocean and climate dynamics in the southeastern tropical Indian Ocean region, particularly in the southeastern of Indian Ocean to the west of Australia.

CRediT authorship contribution statement

Riza Yuliratno Setiawan: Writing – review & editing, Writing – original draft, Visualization, Validation, Methodology, Investigation, Funding acquisition, Formal analysis, Data curation. **R. Dwi Susanto:** Validation, Supervision. **Takanori Horii:** Writing – review & editing, Visualization, Validation, Investigation, Formal analysis, Data curation, Conceptualization. **Inovasita Alifdini:** Software, Formal analysis, Data curation. **Eko Siswanto:** Supervision, Methodology. **Qurnia Wulan Sari:** Writing – original draft. **Anindya Wirasatriya:** Software, Formal analysis. **Candra Aryudiawan:** Resources.

Declaration of competing interest

The authors declare that they have no known competing financial interests or personal relationships that could have appeared to influence the work reported in this paper.

The authors declare the following financial interests/personal relationships which may be considered as potential competing interests:

Riza Yuliratno Setiawan reports financial support was provided by Gadjah Mada University (Rekognisi Tugas Akhir 2021). Riza Yuliratno Setiawan reports financial support was provided by The Ministry of Education and Culture of the Republic of Indonesia (World Class Professor 2023).

Data availability

All data used in this study are free and it can be downloaded via internet

Acknowledgment

This research was funded by grants from Universitas Gadjah Mada (Rekognisi Tugas Akhir 2021; 3143/UN1.P.III/DIT-LIT/PT/2021). RYS acknowledged the travel grant awarded by the World Class Professor 2023 scheme of the Ministry of Education and Culture of the Republic of Indonesia. RDS is also supported by National Aeronautics and Space Administration (NASA) grant #80NSSC18K0777 through the University of Maryland, College Park, USA.

References

Aditya, H.N., Wirasatriya, A. Kunarso, Ismunarti, D.H., Rifai, A., Ismanto, A., Widiaratih, R. 2021. Impact of tropical Cyclones Cempaka and Dahlia to the variability of chlorophyll-a and sea surface temperature in the Seas Southern Coast of Java Island. Eco. Env. Cons. 27, S379-S387.

Akima, H., 1970. A new method of interpolation and smooth curve fitting based on local procedures. J. ACM 17 (4), 589–602. https://doi.org/10.1145/321607.321609.

Atlas, R., Hoffman, R.N., Ardizzone, J., Leidner, S.M., Jusem, J.C., Smith, D.K., Gombos, D., 2011. A cross-calibrated, Multiplatform Ocean surface wind velocity product for meteorological and oceanographic applications. Bull. Am. Meteor. Soc 92 (2), 157–174. https://doi.org/10.1175/2010BAMS2946.1.

Behrenfeld, M.J., Falkowski, P.G., 1997. Photosynthetic rates derived from satellite-based chlorophyll concentration. Limnol. Oceanogr. 42 (1), 1–20. https://doi.org/10.4319/lo.1997.42.1.0001.

Bonjean, F., Lagerloef, G.S.E., 2002. Diagnostic model and analysis of the surface currents in the tropical Pacific Ocean. J. Phys. Oceanogr. 32, 2938–2954. https://doi.org/10.1175/1520-0485(2002)032%3C2938:DMAAOT%3E2.0.CO;2.

Busireddy, N.K.R., Ankur, K., Osuri, K.K., Sivareddy, S., Niyogi, D., 2019. The response of ocean parameters to tropical cyclones in the bay of Bengal. Quart. J. Roy. Meteor. Soc. 145 (724), 3320–3332. https://doi.org/10.1002/qj.3622.

Chen, Y., Tang, D., 2012. Eddy-feature phytoplankton bloom induced by a tropical cyclone in the South China Sea. Int. J. Remote Sens. 33 (23), 7444–7457. https://doi.org/10.1080/01431161.2012.685976.

Demaria, M., Chan, J.C.L. 1984. Comments on "A numerical study of the interactions between Two tropical cyclones". Mon. Wea. Rev. 112, 1643-1645. doi:10.1175/1520-0493(1984)112<1643:CONSOT>2.0.CO;2.

DeMaria, M., Schubert, W.H. 1984. Experiments with a Spectral Tropical Cyclone Model. J. Atmos. Sci. 41(5), 901-924. doi: 10.1175/1520-0469(1984)041<0901:EWASTC>2.0.CO;2.

Dong, K., Neumann, C.J., 1983. On the relative motion of binary tropical cyclones. Mon. Weather Rev. 111 (5), 945–953. https://doi.org/10.1175/1520-0493(1983)111<0945:OTRMOB>2.0.CO;2.

Fu, S.-M., Sun, J.-H., Li, W.-L., Zhang, Y.-C., 2018. Investigating the mechanisms associated with the evolutions of twin extratropical cyclones over the Northwest Pacific Ocean in mid-January 2011. J. Geophys. Res. 123 (8), 4088–4109. https://doi.org/10.1002/2017JD027852.

Fujiwhara, S., 1921. The natural tendency towards symmetry of motion and its application as a principle in meteorology. Quart. J. Roy. Meteor. Soc. 47 (200), 287–292. https://doi.org/10.1002/qj.49704720010.

Fujiwhara, S., 1922. On the growth and decay of vortical system and the mechanism of extratropical cyclones. Jpn. J. Astron. Geophys. 1, 125.

Fujiwhara, S., 1923. On the growth and decay of vortical systems. Quart. J. Roy. Meteor. Soc. 49, 75–104. https://doi.org/10.1002/qj.49704920602.

Fujiwhara, S., 1931. Short note on the behavior of two vortices. Proc. Phys. Math. Soc. Japan 13, 106–110.

Hersbach, H., Bell, B., Berrisford, P., Hirahara, S., Horányi, A., Muñoz-Sabater, J., Nicolas, J., Peubey, C., Radu, R., Schepers, D., Simmons, A., Soci, C., Abdalla, S., Abellan, X., Balsamo, G., Bechtold, P., Biavati, G., Bidlot, J., Bonavita, M., Thépaut, J., 2020. The ERA5 global reanalysis. Quart. J. Roy. Meteor. Soc. 146 (730), 1999–2049. https://doi.org/10.1002/qj.3803.

Hout, Y., Babin, M., Bruyant, F., Grob, C., Twardowski, M.S., Claustre, H., 2007. Does chlorophyll a provide the best index of phytoplankton biomass for primary productivity studies? Biogeosci. Discuss. 4 (2), 707–745. https://doi.org/10.5194/bgd-4-707-2007.

Hsieh, W.W., Boer, G.J., 1992. Global climate change and ocean upwelling. Fis. Oceangr 1, 333–338. https://doi.org/10.1111/j.1365-2419.1992.tb00005.x.

Hung, C.C., Gong, G.C., 2011. Biogeochemical responses in the southern East China Sea after typhoons. Oceanogr 24 (4), 42–51. https://doi.org/10.5670/oceanog.2011.93.

Iskandar, I., Lestari, D.O., Saputra, A.D., Setiawan, R.Y., Wirasatriya, A., Susanto, R.D., Mardiansyah, W., Irfan, M., Rozirwan, Setiawan, J.D., Kunarso. 2022. Extreme Positive Indian Ocean Dipole in 2019 and Its Impact on Indonesia. Sustainability, 14, 15155. doi: 10.3390/su142215155.

Islamiyah, K., Ngurah Suarbawa, K., Sumaja, K., 2023. Effect of tropical cyclones on high waves in the southern regions of Java, Bali, and Nusa Tenggara (case study of tropical cyclones Claudia). Bul. Fisik. 24 (1), 54–60. https://www.researchgate.net/publication/359909812.

Ito, K., Hirano, S., Lee, J.-D., Chan, J.C.L., 2023. Three-dimensional Fujiwhara effect for binary tropical cyclones in the Western North Pacific. Mon. Weather Rev. 151 (7), 1779–1795. https://doi.org/10.1175/MWR-D-22-0239.1.

Knutson, T., Camargo, S.J., Chan, J.C.L., Emanuel, K., Ho, C.H., Kossin, J., Mohapatra, M., Satoh, M., Sugi, M., Walsh, K., Wu, L., 2020. Tropical cyclones and climate change assessment part II: projected response to anthropogenic warming. Bull. Am. Meteorol. Soc. 101 (3), E303–E322. https://doi.org/10.1175/BAMS-D-18-0194.1.

Lee, J.-D., Ito, K., Chan, J.C.L., 2023. Importance of self-induced vertical wind shear and diabatic heating on the Fujiwhara effect. Quar. J. Roy. Meteor. Soc. 149 (753), 1197–1212. https://doi.org/10.1002/qj.4448.

Lee, J.-H., Moon, J.-H., Kim, T., 2020. Typhoon-triggered phytoplankton bloom and associated Upper-Ocean conditions in the northwestern Pacific: evidence from satellite remote sensing, Argo profile, and an ocean circulation model. J. Mar. Sci. Eng. 8 (10), 788. https://doi.org/10.3390/jmse8100788.

Lin, I., Liu, W.T., Wu, C.-C., Wong, G.T.F., Hu, C., Chen, Z., Liang, W.-D., Yang, Y., Liu, K.-K., 2003. New evidence for enhanced ocean primary production triggered by tropical cyclone. Geophys. Res. Lett. 30 (13) https://doi.org/10.1029/2003GL017141.

Liou, Y.A., Pandey, R.S., 2020. Interactions between typhoons Parma and Melor (2009) in north West Pacific Ocean. Wea. Clim. Extrem. 29 https://doi.org/10.1016/j.wace.2020.100272.

Liou, Y.A., Liu, J.-C., Liu, C.-C., Chen, C.-H., Nguyen, K.-A., Terry, J.P., 2019. Consecutive dual-Vortex interactions between quadruple typhoons Noru, Kulap, Nesat and Haitang during the 2017 North Pacific typhoon season. Remote Sens. 11 (16), 1843. https://doi.org/10.3390/rs11161843.

Liu, F., Tang, S., 2018. Influence of the interaction between typhoons and oceanic mesoscale eddies on phytoplankton blooms. J. Geophys. Res. 123 (4), 2785–2794. https://doi.org/10.1029/2017JC013225.

Liu, L., 2013. Effect of wind-current interaction on ocean response during typhoon KAEMI (2006). Sci. China Earth Sci. 56 (3), 418–433. https://doi.org/10.1007/s11430-012-4548-3.

Mandal, S., Susanto, R.D., Ramakrishnan, B., 2022. On Investigating the Dynamical Factors Modulating Surface Chlorophyll-a Variability along the South Java Coast. Rem. Sens. 14, 1745. https://doi.org/10.3390/rs14071745.

Murakami, H., 2016. In: Frouin, R.J., Shenoi, S.C., Rao, K.H. (Eds.), Ocean color estimation by Himawari-8/AHI, p. 987810. https://doi.org/10.1117/12.2225422.

Nugroho, S.C., Setiawan, R.Y., Setiawati, M.D., Djumanto, Priyono, S.B, Susanto, R.D., Wirasatriya, A., Larasati, R.F., 2023. Estimation of albacore tuna potential fishing grounds in the southeastern Indian Ocean. IEEE Access 11, 1141–1147. https://doi.org/10.1109/ACCESS.2022.3233353.

Pandey, R.S., Liou, Y.A., Liu, J.C., 2021. Season-dependent variability and influential environmental factors of super-typhoons in the Northwest Pacific basin during 2013-2017. Wea. Clim. Extrem. 31 https://doi.org/10.1016/j.wace.2021.100307.

Paterson, L. 2012. Tropical Low AU1011_01U (Anggrek). Bur. Meteorology. Australia. Accessed: May 28, 2024. [Online]. Available: http://www.bom.gov.au/cyclone/history/pdf/anggrek.pdf.

Roxy, M.K., Modi, A., Murtugudde, R., Valsala, V., Panickal, S., Prasanna, S., Ravichandran, M., Vichi, M., Lévy, M., 2016. A reduction in marine primary productivity driven by rapid warming over the tropical Indian Ocean. Geophys. Res. Lett. 43 (2), 826–833. https://doi.org/10.1002/2015GL066979.

Samodra, G., Ngadisih, N., Malawani, M.N., et al., 2020. Frequency–magnitude of landslides affected by the 27–29 November 2017 Tropical Cyclone Cempaka in Pacitan, East Java. J. Mt. Sci. 17, 773–786. https://doi.org/10.1007/s11629-019-5734-y.

Setiawan, R.Y., Susanto, R.D., Wirasatriya, A., Alifdini, I., Puryajati, A.D., Maslukah, L., Nurdin, N., 2021. Impacts of tropical cyclone Seroja on the phytoplankton chlorophyll-a and sea surface temperature in the Savu Sea, Indonesia. IEEE Access 9, 152938–152944. https://doi.org/10.1109/ACCESS.2021.3125605.

Sharma, S., Ha, K.J., Yamaguchi, R., Rodgers, K.B., Timmermann, A., Chung, E.S., 2023. Future Indian Ocean warming patterns. Nat. Commun. 14 (1), 1789. https://doi.org/10.1038/s41467-023-37435-7.

Siswanto, E., Ishizaka, J., Morimoto, A., Tanaka, K., Okamura, K., Kristijono, A., Saino, T., 2008. Ocean physical and biogeochemical responses to the passage of typhoon Meari in the East China Sea observed from Argo float and multiplatform satellites. Geophys. Res. Lett. 35 (15), 1–5. https://doi.org/10.1029/2008GL035040.

Stewart, R.H., 2008. Introduction to Physical Oceanography. Texas A & M University, Texas, USA.

Susanto, R.D., Gordon, A.L., Zheng, Q., 2001. Upwelling along the coasts of Java and Sumatra and its relation to ENSO. Geophys. Res. Lett. 28 (8), 1599–1602. https://doi.org/10.1029/2000GL011844.

Suzuki, S.-I., Niino, H., Kimura, R., 2011. The mechanism of upper-oceanic vertical motions forced by a moving typhoon. Fluid Dyn. Res. 43, 1–24. https://doi.org/10.1088/0169-5983/43/2/025504.

The, W.G., 1988. The WAM model-A third generation ocean wave prediction model. J. Phys. Oceanogr. 18, 1775–1810. https://doi.org/10.1175/1520-0485(1988)018%3C1775:TWMTGO%3E2.0.CO;2.

Wang, Y., 2020. Composite of typhoon-Induced sea surface temperature and chlorophyll-a responses in the South China Sea. J. Geophys. Res. 125 (10) https://doi.org/10.1029/2020JC016243.

Wang, J-J., Tang, D.L., 2014. Phytoplankton patchiness during spring intermonsoon in western coast of South China Sea. Deep Sea Res. II, 101, 120–128. https://doi.org/10.1016/j.dsr2.2013.09.020.

Windupranata, W., Nusantara, A.D.S., Wijaya, D., Prijatna, K., 2019. Impact analysis of tropical cyclone Cempaka-Dahlia on Wave Heights in Indonesian waters from numerical model and altimetry satellite. KnE Eng. 4 (3), 203–214. https://doi.org/10.18502/keg.v4i3.5851.

Wirasatriya, A., Setiawan, J.D., Sugianto, D.N., Rosyadi, I.A., Haryadi, H., Winarso, G., Setiawan, R.Y., Susanto, R.D., 2020. Ekman dynamics variability along the southern coast of Java revealed by satellite data. Int. J. Remote Sens. 41 (21), 8475–8496. https://doi.org/10.1080/01431161.2020.1797215.

Wu, R., Yang, Q., Tian, D., Han, B., Wu, S., Zhang, H., 2019. Response of coastal water in the Taiwan Strait to typhoon Nesat of 2017. Water 11 (11), 2331. https://doi.org/10.3390/w11112331.

Zhang, H., Liu, X., Wu, R., Chen, D., Zhang, D., Shang, X., Wang, Y., Song, X., Jin, W., Yu, L., Qi, Y., Tian, D., Zhang, W., 2020. Sea surface current response patterns to tropical cyclones. J. Mar. Syst. 208 https://doi.org/10.1016/j.jmarsys.2020.103345.

Yang, Y., Liu, L., Liu, K., Yu, W., Wang, H., 2020. Diurnal Sea surface temperature response to tropical cyclone Dahlia in the Eastern tropical Indian Ocean in 2017 revealed by the Bailong buoy. Dyn. Atmos. Oceans. 92 https://doi.org/10.1016/j.dynatmoce.2020.101163.

Zhang, H., He, H., Zhang, W.Z., Tian, D., 2021. Upper Ocean response to tropical cyclones: a review. Geosci. Lett. 8, 1–12. https://doi.org/10.1186/s40562-020-00170-8.

Zhao, H., Tang, D., Wang, Y., 2008. Comparison of phytoplankton blooms triggered by two typhoons with different intensities and translation speeds in the South China Sea. Mar. Ecol. Prog. Ser. 365, 57–65. https://doi.org/10.3354/meps07488.

Zhao, H., Han, G., Zhang, S., Wang, D., 2013. Two phytoplankton blooms near Luzon Strait generated by lingering typhoon Parma. Eur. J. Vasc. Endovasc. Surg. 118 (2), 412–421. https://doi.org/10.1002/jgrg.20041.

Zhao, H., Shao, J., Han, G., Yang, D., Lv, J., 2015. Influence of typhoon Matsa on phytoplankton chlorophyll-A off East China. PLoS One 10 (9), e0137863. https://doi.org/10.1371/journal.pone.0137863.